

## Study of bone cells by quantitative phase microscopy using a Mirau interferometer

J. González-Laprea<sup>a,\*</sup>, A. Márquez<sup>b</sup>, K. Noris-Suárez<sup>b</sup>, and R. Escalona<sup>a</sup>

<sup>a</sup>Laboratorio de Óptica e Interferometría, Departamento de Física.

\*Laboratorio de Óptica e Interferometría (006), Edificio de Física y Electrónica I, Universidad Simón Bolívar,  
Carretera Baruta - Hoyo de la Puerta, valle de Sartenejas, Caracas, 1080-A, Venezuela,

Tel: +58 212 906 3522; Fax: +58 212 906 3600

e-mail: jeglaprea@usb.ve

<sup>b</sup>Laboratorio de Bioingeniería de tejidos Departamento de Biología Celular,  
Universidad Simón Bolívar (Venezuela).

Recibido el 25 de octubre de 2010; aceptado el 16 de agosto de 2011

The article presents the use of an interference microscope, using a Mirau objective for the study of the early adhesion process of osteoblast-like bone cells, using the phase shifting technique. The process is carried out on surgical stainless steel surfaces of interest for the development of bone implants. Experimental phase maps are directly related to cell profiles. These phase maps are obtained for several adhesion times, which indicate morphological changes in cells. Mainly the change in height profiles through time and the interaction with other surrounding cells are observed. The experimental system used is appropriate for the time scales observed, in the order of hours, showing strength and precision in the calculation of the optical phase.

**Keywords:** Interferential microscopy; optical phase maps; osteoblast-like cells; quantitative phase microscopy; opaque surfaces.

El artículo presenta el uso de un microscopio interferencial, empleando un objetivo de Mirau, para el estudio del proceso de adhesión temprana de células óseas tipo osteoblasto, por medio de la técnica de desplazamiento de fase. El proceso es llevado a cabo sobre superficies de acero quirúrgico, que son de interés en el desarrollo de prótesis óseas. Los mapas de fase óptica obtenidos a diversos tiempos de adhesión muestran cambios morfológicos en las células; principalmente se observa el cambio en la altura de los perfiles de la fase a través del tiempo y la formación de conexiones intercelulares. El sistema de medición empleado es apropiado para las escalas de tiempo de evolución exhibidas por el sistema celular (del orden de horas), presentando además alta robustez y precisión en el cálculo de la fase óptica.

**Descriptores:** Microscopía interferencial; mapas de fase óptica; células osteoblasto; microscopía de fase cuantitativa; superficies opacas.

PACS: 42.87.Bg; 87.17.Ee

### 1. Introduction

The process of early adhesion of an osteoblast-like bone cell is characterized by a morphologic change in the cell, which passes from a spheroid form when the cell is in suspension, to a flat morphology with straight edges when it is already adhered to the surface of the material. Difficulties affecting the cells through this stage could condition their subsequent function in the remaining cell processes both *in-vitro* and *in vivo* (proliferation, differentiation or apoptosis, as appropriate). To evaluate this limiting step is fundamental in the characterization of potential materials for bone prostheses (Chapekar, 1996; Johnson, *et al.*, 1985; Ratner, Hoffman, Schoen, & Lemons, 2004).

Optical microscopy is generally used in the study of *in-vitro* morphology. Even though the cells are basically transparent to visible light, the elements that constitute the cytosol, as well as the organelle contained inside the cell, gives the cells a different refractive index from their surrounding environment, which turns them fundamentally into phase objects (Barone-Nugent, Barty, & Nugent, 2002; Curl, *et al.*, 2006; Murphy, 2001; Popescu, Park, Lue, *et al.*, 2008). Such techniques as phase contrast or differential interference contrast (DIC) are widely used in biomedical research laboratories

because they allow translating the information of the optical phase to light intensities. These techniques present two basic drawbacks: first it is not possible to obtain quantitative data of the optical phase from the values of intensity because there is no a simple relationship between both variables. Second, they generally require different elements in the objective and the light condenser of the optical system, and therefore they must be implemented in transmitted light systems and not incident light (reflection); in this case, they are not applicable on opaque surfaces (Bennett, Jupnik, Osterberg, & Richards, 1951; Danz & Gretscher, 2004; Murphy, 2001).

The use of optical techniques in cellular systems has been increasingly implemented in the last decade for the quantitative study from the optical phase, since it provides information about the morphology and the refractive index of the cell throughout the optical axis (Barone-Nugent, *et al.*, 2002; Curl, *et al.*, 2004; Popescu, Park, Lue, *et al.*, 2008; Popescu, Park, Choi, *et al.*, 2008). The present work shows the implementation of a system of interferential microscopy by phase shifting, and its viability for the study of the process of early adhesion of bone osteoblast-like cells on opaque surfaces, in order to evaluate cellular processes *in-vitro* with the cells in viable conditions and without later modifications such as treatments of fixation or chemical staining procedures, which

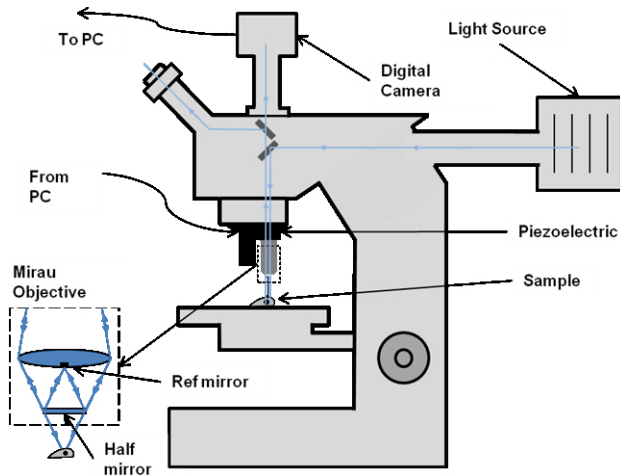


FIGURE 1. Schematic of the incident light microscope. In detail, the interferential objective.

can induce modifications in the cellular preparations and hence significantly alter the parameters being studied (Hayat, 2004; Romero, Sánchez, Rodríguez, González, & Suarez, 2009).

## 2. Materials and methods

### 2.1. Mirau interferometer

In a Mirau interferometer, the light originating from the source goes through a partially reflecting mirror which acts as the reference surface; the transmitted beam is reflected by the sample to later interfere with the reference beam. This simple design allows the manufacture of objectives with the interferometer in its interior (Fig. 1), which makes the system very stable under mechanical or thermal disturbances (Hariharan, 2003). This compact interferometer is used generally in the study of polished surfaces or those with small variations in their topography (Ge & Kobayashi, 2006). This way, cells like the osteoblasts which are thin and with refractive indices similar to the one of their surrounding environment can suitably be studied with this device.

### 2.2. Optical microscopy system

The interferential microscope consists of a conventional Nikon Optiphot microscope of incident light frequently used for metallurgical applications which employs a 20X Mirau type interferential objective. The illumination comes from a tungsten lamp with an interferential filter centered at  $\lambda$  546,1 nm wavelength, and a spectral bandwidth of 10 nm. The trinocular head of the microscope allows for simultaneously obtaining an image for the observer and another for a digital camera, which allows for control of the system and the acquisition of digital interferograms (Fig. 1). To obtain the optical phase, the phase shifting technique is used. This shifting is carried out by means of a piezoelectric transducer

that replaces the traditional support of objectives in the microscope (Gåsvisk, 2002; Hariharan, 2003). The control of the piezoelectric system carries out by means of a frequency-to-voltage circuit converter made in our laboratory, connected to a conventional pc sound card. The performance of this homemade controller to drive phase shifting is equal or superior to than obtained with a 16 bit analogic-digital converter (González-Laprea, Cappelletto, & Escalona, 2010). The phase reconstructions are realized introducing an arbitrary optical phase in five steps of  $\alpha_i = \pi/2$  rad. The optical phase is experimentally determined from the five acquisitions using the relation:

$$\Phi(x, y) = \arctan \left( \frac{2(I_4 - I_2)}{I_1 - 2I_3 + I_5} \right) \quad (1)$$

where the  $I_n$  are the intensity values at each point of the interferogram ( $I(x, y)$ ) for each increases of  $\alpha_i$ . Although the technique of phase shifting requires acquisition times greater than those of other techniques, these times continue being very small in comparison to the evolution times of our biological system under study. Additionally, it has been demonstrated that redundant information in the methodology of 5 buckets reduces the effect of errors committed in the introduction of the optical phase. (Kinnstaetter, Lohmann, Schwider, & Streibl, 1988; Van Wingerden, Frankena, & Smorenburg, 1991). Phase unwrapping is carried out following an iterative technique according to the branchcut algorithm. (Venema & Schmidt, 2008; Wang & Li, 1999).

Once the optical phase  $\Phi(x, y)$  is experimentally determined through Eq. (1), the topographical cell profiles  $H(x, y)$  are directly related to  $\Phi(x, y)$  by means of the following relationship,

$$H(x, y) = \frac{\lambda \Phi(x, y)}{4\pi n_{cel}} \quad (2)$$

where  $\lambda$  is the wavelength of illuminating light and  $n_{cel}$  is the mean refractive index of the cells, assumed nearly constant in this study. (Creath & Wyant, 1990).

### 2.3. Cellular system

The osteoblasts are bone cells responsible for the regenerative process of that tissue, in which they take part secreting the organic component of the extracellular matrix after adhesion to its substrate. *In-vitro* these cells are characterized by the formation of mono-layers of interconnected cells to each other, presenting cells of cuboids morphologies with thicknesses under a few micrometers. For this study the bone cells were obtained from calvaria (parietal and frontal bones from the skull of 2-3 days newborn rats *Sprague Dowley*), following the methodology described by Noris-Suárez *et al.*, (Noris-Suarez, *et al.*, 2003). Once the soft tissue is eliminated (by scrapping), the calvaria were cut in pieces of around 1 mm<sup>2</sup> and submitted to a digestion process using 0.1 mg collagenase, 0.25 mg trypsin, 0,5 mM EDTA in a D-MEM culture medium. Incubations were performed by means of three series incubating to 37°C by 20 minutes in smooth agitation, and cells collected from third extraction process were

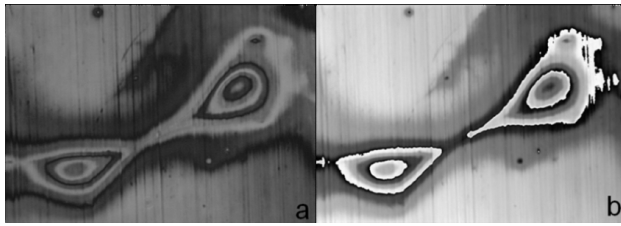


FIGURE 2. a) Interferograms corresponding to a pair of cells interacting after 24.5 hours of seeding. b) Wrapped phase map reconstruction obtained from interferograms. Interferograms shows a difference between their maximum and minimum of intensity superior at the one hundred gray level.

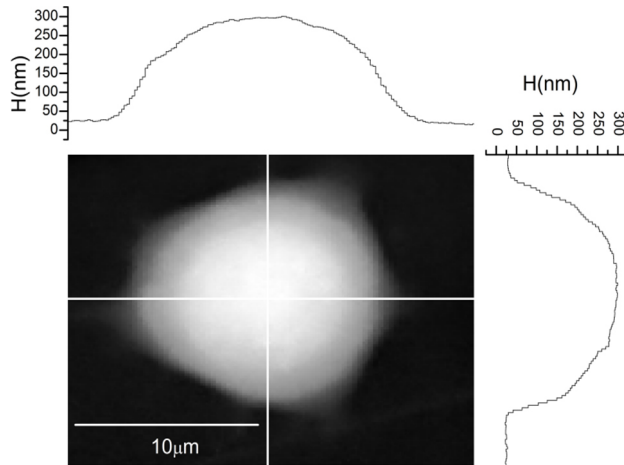


FIGURE 3. Osteoblast topographic map in gray levels, after  $(2.5 \pm 0.3)$  hours of culture on 316LVM steel. The lateral plots correspond to the profiles throughout the white drawn up lines. A cross section of about  $100 \mu\text{m}^2$  can be observed approximately and a maximum height of nearly 300 nm for the osteoblast.

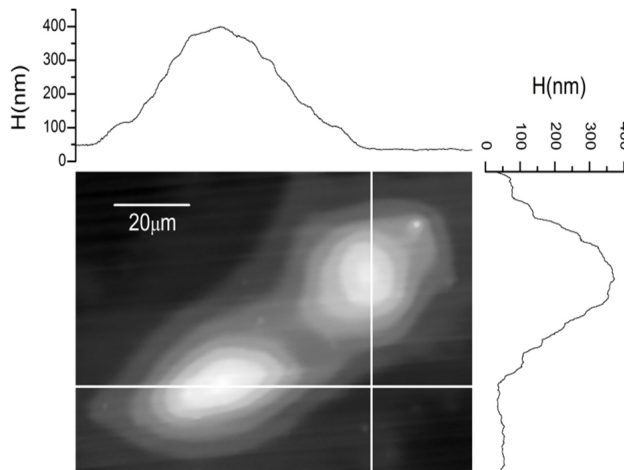


FIGURE 4. Topographic map in gray scale levels, osteoblast after  $(7.0 \pm 0.3)$  hours of culture on 316LVM steel. Lateral plots correspond to the profiles throughout the white drawn up lines. A cross section of about  $300 \mu\text{m}^2$  can be observed approximately and a peak height of about 400 nm.

plated in culture plates of 100 mm of diameter in the D-MEM medium complemented with 10% fetal bovine serum, 100  $\mu\text{g}/\text{mL}$  of penicillin (200,000 U/mL) and streptomycin

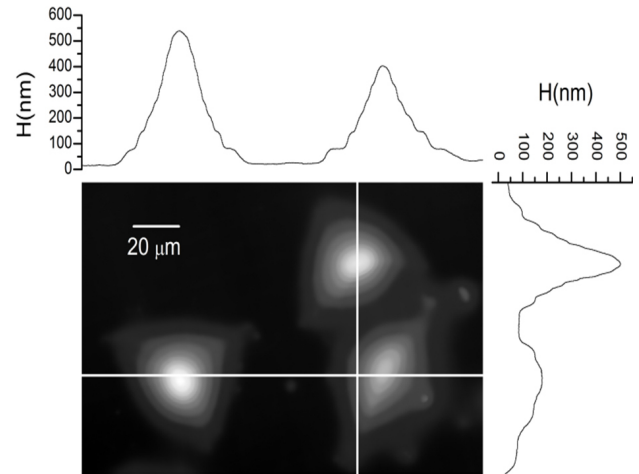


FIGURE 5. Topographic map in gray scale levels, osteoblast after  $(9.3 \pm 0.3)$  hours of culture on 316LVM steel. Lateral plots correspond to the profiles throughout the white drawn up lines. A cross section of about  $300 \mu\text{m}^2$  can be observed approximately for the osteoblast and a peak height of some 500 nm.

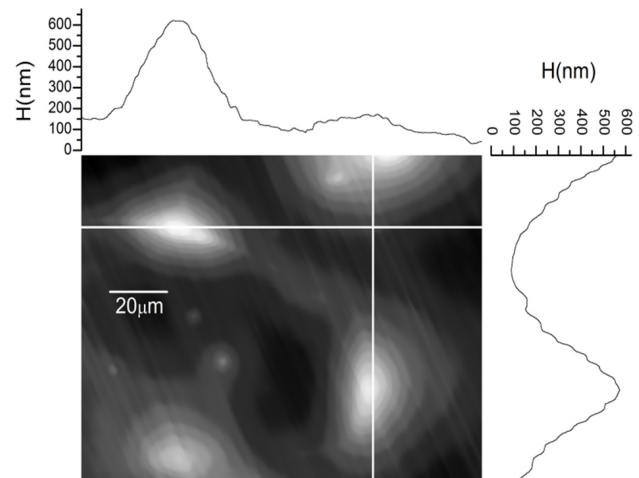


FIGURE 6. Topographic map in gray scale levels, osteoblast after  $(14.3 \pm 0.3)$  hours of culture on 316LVM steel. Lateral plots correspond to the profiles throughout the white drawn up lines. The cells begin to form interconnections, links which are nearly visible in the phase map.

(200,000 U/mL), nonessential amino acids and L-glutamine. The culture plates were cultivated in atmosphere of appropriate  $\text{CO}_2$  and humidity and the media were changed every 3 or 4 days (Noris-Suarez, *et al.*, 2003).

In order to evaluate the cellular adhesion on the 316LVM stainless steel, discs of this material with approximately 1 cm diameter were worked with mechanical polishing until obtaining an average roughness around to  $0.15 \mu\text{m}$ . In order to study individual sets of cells, approximately  $3 \times 10^3$  cells/ $\text{cm}^2$  were plated, in order to have a relatively low proportion of cells, compared with  $20 \times 10^3$  cells/ $\text{cm}^2$  that are used generally when cellular confluence is desired (Noris-Suarez, *et al.*, 2003). Also, a test seeding of  $10^3$  cells/ $\text{cm}^2$  was performed

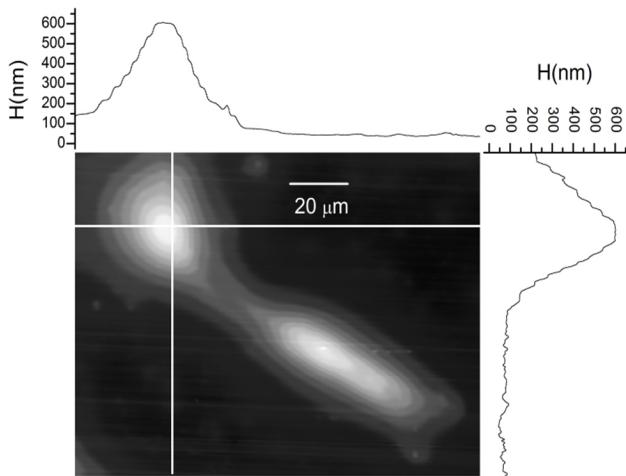


FIGURE 7. Topographic map in gray scale levels, osteoblast after  $(16.6 \pm 0.3)$  hours of culture on 316LVM steel. Lateral plots correspond to profiles throughout the white drawn up lines. The process of interconnection between the cells can be clearly observed.

to see the effects of cell isolation on their morphology. The cells were studied in a lapse up to 25 hours after the seeding.

### 3. Results and discussion

The cells sown on steel discs were placed in the interferential microscope for their study in the subsequent hours. Figure 2 shows a typical interferogram under study and the corresponding wrapped phase map, corresponding to a pair of cells interacting after 24.5 hours of seeding.

Diverse osteoblasts cultures were carried out under the same conditions (95% of humidity and 5% of  $\text{CO}_2$ ) allowing to observe the modifications of the cells according to their evolution times. Figures 3 to 8 correspond to images in gray scale levels related to the topography of the cells, where we have assumed a homogeneous refractive index average for the cell of  $n_{cel} = 1.360$ . (Curl, *et al.*, 2005; Rappaz, *et al.*, 2005). The height at each point ( $H(x, y)$ ) of a phase object (in our case the cell) as a function of the optical phase is given by Eq. (2).

It is possible to observe in Fig. 3 that after 2.5 hours of culture, the cell already begins to present the straight edges characteristic of its cuboid morphology, even though it maintains its reminiscent spherical profile of its state in solution (spheroid form). After 7 hours of seeding the cells appear extended, spanning a larger surface. In addition, it can be observed how the cell profiles become narrower, implying the loss of their spheroid form, as shown in Figs. 4 and 5.

At later times, it is possible to observe not only how the cells follows its process of adhesion but also how it begins to form the interconnections with the purpose of to establish the cell monolayer (Figs. 6, 7 and 8). This process is characteristic of these cell types that require establishing connections with their pairs in order to be able to realize other functions such as the secretion of extracellular matrix and cellular signaling processes.

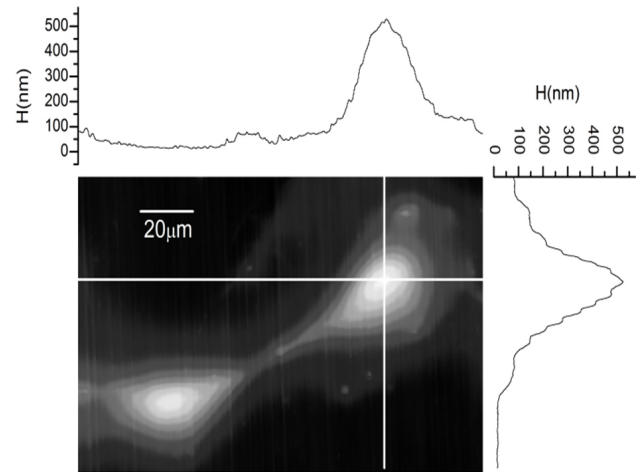


FIGURE 8. Topographic map in gray scale levels, osteoblast after  $(23.3 \pm 0.3)$  hours of culture on 316LVM steel. Lateral plots correspond to the profiles throughout the drawn up lines. Straight edges and interconnections between the cells can be observed.

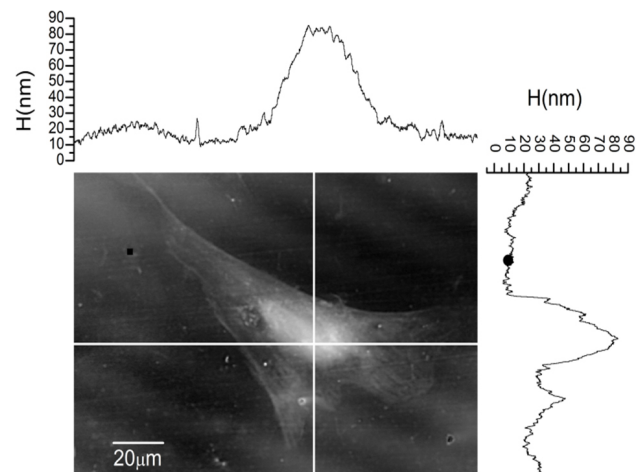


FIGURE 9. Topographic map in gray scale levels, osteoblast after  $(16.5 \pm 0.3)$  hours of culture on 316LVM steel. Lateral plots correspond to the profiles throughout the white drawn up lines. Height loss at nucleus position suggests non ideal conditions for the physiological functions of the cell.

Figures 3 to 8 allow us to observe and analyze how the cell adheres on the substrate as time passes. Although the maximum height parameter in the cell does not change significantly between the figures (this effect can be attributed to the presence of the cellular nucleus in this region), the fact that the profile becomes narrower indicates that the cell spreads gradually on the surface (Ratner, *et al.*, 2004).

When cells are sown in smaller density ( $10^3$  cel/cm<sup>2</sup> as it was described in preceding section), the cultures exhibits a low number of cells so that it prevents them to making contact and interacting between them. Therefore it is possible to observe in Fig. 9 how the cell increase its cross section (spread), reaching larger lateral dimensions than the cells in semi confluent cultures This behavior can be compared with other cells with similar time evolution (16 hours in Fig. 7).

The height loss suggests that a deformation of the cellular nucleus is happening, since measurements in other conditions show a constant value of this parameter. It can be inferred that this constant value corresponds to the characteristic height of the cell nucleus placed over 316LVM steel. The morphologic changes shown in Fig. 9 suggest that cells are in a state that is not optimal for a suitable development of their biological functions. (Haber & Thilly, 1978; Yalcin, Perry, & Ghadiali, 2007).

#### 4. Conclusions

We have presented the implementation of a Mirau interferential microscopy technique for the study of cellular systems employing bone osteoblast-like cells, of great interest in the development of materials for bone implant. This microscopy technique constitutes an extremely useful tool for the study of this type of cells, since it allows for the analysis of the dynamics of adhesion and early interaction with the substrate and other cells *in vitro*. Also the present technique allows for observation of morphologic variations in the cells as well

as the establishment of early interconnections that favor the formation of a cellular monolayer an effect that is not easily observable with other optical microscopy techniques. In the same way, the fact of being able to observe cellular morphology on an opaque surface, is of extreme utility to evaluate the proliferation of cells on any material of interest, even more if it is considered that these cells are still alive during the observation process and they have not been previously submitted to any dehydration or another fixation treatment for microscope observation, like the required ones for others microscope techniques, that could modify their morphologic characteristics.

#### Acknowledgments

This work was supported by FONACIT-Venezuela, Research Project Number G-1997000593, by FONACIT-Venezuela, Misión Ciencia Fellowship and Simón Bolívar University, Research Group Project USB DID-GID61. Tanks to the Materials Lab from the Venezuelan institute for the scientific research by the steel discs provided.

- 
1. E.D. Barone-Nugent, A. Barty, and K.A. Nugent, Quantitative phase-amplitude microscopy I: optical microscopy. *Journal of Microscopy* **206** (2002) 194-203.
  2. A.H. Bennett, H. Jupnik, H. Osterberg, and O.W. Richards, *Phase Microscopy: Principles and Applications*. (New York: John Wiley and Sons, Inc. 1951)
  3. K. Creath, and J.C. Wyant, Absolute measurement of surface roughness. *Applied Optics* **29** (1990) 3823-3827.
  4. C.L. Curl *et al.*, Single Cell Volume Measurement by Quantitative Phase Microscopy (QPM): A Case Study of Erythrocyte Morphology. *Cellular Physiology and Biochemistry* **17** (2006) 193-200.
  5. C.L. Curl, *et al.*, Refractive Index Measurement in Viable Cells Using Quantitative Phase-Amplitude Microscopy and Confocal Microscopy. *Cytometry Part A* **65** (2005) 88-92.
  6. C.L. Curl, *et al.*, Quantitative phase microscopy: a new tool for measurement of cell culture growth and confluency *in situ*. *European Journal of Physiology* **448** (2004) 462-468.
  7. M.S. Chapekar, Regulatory concerns in the development of biologic-biomaterial combinations. *Journal of Biomedical Materials Research*. **33** (1996) 199-203.
  8. R. Danz, and P. Gretscher, C-DIC: a new microscopy method for rational study of phase structures in incident light arrangement. *Thin Solid Films* **462-463** (2004) 257-262.
  9. K.J. Gåsvik, *Optical Metrology* (3<sup>rd</sup> ed. West Sussex, England: John Wiley and Sons Ltd. 2002)
  10. Z. Ge, and F. Kobayashi, High-precision measurement of a fiber connector end face by use of a Mirau interferometer. *Applied Optics* **45** (2006) 5832-5839.
  11. J. González-Laprea, J. Cappelletto, and R. Escalona, Using a frequency to voltage converter as a phase controller in phase shifting interferential microscopy. *International Journal of Optomechatronics* **5** (2011) 68-79.
  12. D.A. Haber and W.G. Thilly, Morphological transformation of C3H/10T1/2 cells subcultured at low cell densities. *Life Science* **22** (1978) 1663-1673.
  13. P. Hariharan, *Optical Interferometry* (2<sup>da</sup> ed. Amsterdam: Academic Press. 2003)
  14. M.A. Hayat, *Principles and techniques of Electron Microscopy, Biological applications* (4 ed. Cambridge, U.K. Cambridge University Press. 2004)
  15. Johnson, H.J., Northup *et al.*, Biocompatibility test procedures for materials evaluation *in vitro*. II. Objective methods of toxicity assessment. *Journal of Biomedical Materials Research*. **19** (1985) 489-508.
  16. K. Kinnstaetter, A.W. Lohmann, J. Schwider, and N. Streibl, Accuracy of phase shifting interferometry. *Applied Optics* **27** (1988) 5082-5089.
  17. D.B. Murphy, *Fundamentals of Light Microscopy and Electronic Imaging* (1 ed. EE. UU. Wiley-Liss, Inc. 2001)
  18. Noris-Suarez *et al.*, Caracterización biológica empleando células osteoblásticas de vidrios del sistema SiO<sub>2</sub>.Na<sub>2</sub>O.CaO. K<sub>2</sub>O.MgO.P<sub>2</sub>O<sub>5</sub>, Modificados con Al<sub>2</sub>O<sub>3</sub> B<sub>2</sub>O<sub>3</sub>. *Revista latinoamericana de metalurgia y materiales* **23** (2003) 82-88.
  19. Popescu *et al.*, Optical imaging of cell mass and growth dynamics. *Am J Physiol Cell Physiol* (2008) **295** 538-544.
  20. G. Popescu, Y.K. Park, W. Choi, R.R. Dasari, M.S. Feld, and K. Badizadegan, Imaging red blood cell dynamics by quantitative phase microscopy. *Blood Cells, Molecules, and Diseases* **41** (2008) 10-16.

21. B. Rappaz, P. Marquet, E. Cuche, Y. Emery, C. Depeursinge, and P.J. Magistretti, Measurement of the integral refractive index and dynamic cell morphometry of living cells with digital holographic microscopy. *Optics Express* **13** (2005) 9361-9373.
22. B.D. Ratner, A.S. Hoffman, F.J. Schoen, and J.E. Lemons, *Bio-materials science: an introduction to materials in medicine* (2<sup>nd</sup> ed. San Diego, California: Elsevier Academic Press, 2004).
23. M.A. Romero, F. Sánchez, J.P. Rodríguez, G. González, and K N. Suarez, *Evaluación de la interacción celular sobre guías nerviosas mediante MEB comparando dos métodos de secado*. Paper presented at the 10° Congreso Interamericano de Microscopía Electrónica, Rosario, Argentina, 2009).
24. J. Van Wingerden, H.J. Frankena, and C. Smorenburg, Linear approximation for measurement errors in phase shifting interferometry. *Applied Optics* **30** (1991) 2718-2729.
25. T.M. Venema, and J.D. Schmidt, Optical phase unwrapping in the presence of branch points. *Optics Express* **16** (2008) 6985-6998.
26. Z. Wang, and S. Li, Optical phase unwrapping in the presence of branch points. *Applied Optics* **38** (1999) 805-814.
27. H.C. Yalcin, S.F. Perry, and S.N. Ghadiali, Influence of airway diameter and cell confluence on epithelial cell injury in an in vitro model of airway reopening. *Journal of Applied Physiology* **103** (2007) 1796-1807.